Published in final edited form as:
Blood. 2012 April 26; 119(17): . doi:10.1182/blood-2011-09-382556.

Terminal transport of lytic granules to the immune synapse is mediated by the kinesin-1/Slp3/Rab27a complex

Mathieu Kurowska[1,2,3], **Nicolas Goudin**[2,3], **Nadine T. Nehme**[1,2,3], **Magali Court**[4,5,6], **Jérôme Garin**[4,5,6], **Alain Fischer**[1,2,3,7], **Geneviève de Saint Basile**[#1,2,3,7], and **Gaël Ménasché**[#1,2,3]

[1]Inserm, Unité U768, Laboratoire du Développement Normal et Pathologique du Système Immunitaire, Paris, France

[2]Inserm, Institut Fédératif de Recherche Necker Enfants-Malades (IFR94), Université Paris Descartes, Paris, France

[3]Imagine Institute, Paris, France

[4]Inserm, Unité U1038, Grenoble, France

[5]Commisariat à l'énergie atomique, Direction des sciences du vivant, Institut de Recherches en technologies et science du vivant, Laboratoire de Biologie à Grandes Echelle, Grenoble, France

[6]Université Joseph Fourier, Grenoble, France

[7]Assistance Publique–Hôpitaux de Paris, Hôpital Necker Enfants-Malades, Unité d'Immunologie-Hématologie Pédiatrique, Paris, France

[#] These authors contributed equally to this work.

Abstract

Cytotoxic T lymphocytes kill target cells via the polarized secretion of cytotoxic granules at the immune synapse. The lytic granules are initially recruited around the polarized microtubule-organizing center. In a dynein-dependent transport process, the granules move along microtubules toward the microtubule-organizing center in the minus-end direction. Here, we found that a kinesin-1–dependent process is required for terminal transport and secretion of polarized lytic granule to the immune synapse. We show that synaptotagmin-like protein 3 (Slp3) is an effector of Rab27a in cytotoxic T lymphocytes and interacts with kinesin-1 through the tetratricopeptide repeat of the kinesin-1 light chain. Inhibition of the Rab27a/Slp3/kinesin-1 transport complex impairs lytic granule secretion. Our data provide further molecular insights into the key functional and regulatory mechanisms underlying the terminal transport of cytotoxic granules and the latter's secretion at the immune synapse.

Correspondence: Gaël Ménasché, Inserm U768–Développement Normal et Pathologique du Système Immunitaire, Hôpital Necker Enfants-Malades Batiment Pasteur, Porte P2, 149 rue de Sèvres, F-75015 Paris, France; gael.menasche@inserm.fr. .

Authorship Contribution: G.M. designed and conducted most of the experiments with the assistance of M.K.; N.G. contributed to the TIRF experiment; M.C. and J.G. performed the mass spectrometry analysis; N.T.N. contributed to the degranulation assay; G.M. designed the research; and G.M., G.d.S.B., and A.F. wrote the paper.

Conflict-of-interest disclosure: The authors declare no competing financial interests.

The online version of this article contains a data supplement.

Europe PMC Funders Author Manuscripts

Introduction

Cytotoxic T lymphocytes (CTLs) provide a critical means of defense against tumor cells and virus-infected cells. The CTLs' cytotoxic activity is exerted by the secretion of perforin-containing lytic granules at the immune synapse (IS) with the target cell.[1-3] On recognition of the antigen-presenting target cell by the CTL, the microtubule-organizing center (MTOC) reorients toward the target and delivers polarized lytic granules to the plasma membrane at the central supramolecular activation cluster (cSMAC). The cSMAC is surrounded by a ring of adhesion molecules and an actin cytoskeleton, which delimits the peripheral supramolecular activation cluster (pSMAC).[4] The microtubule network is polarized with respect to the MTOC, with "minus" ends directed inward and "plus" end directed outward. Furthermore, 2 sets of microtubules have been described in CTLs conjugated to target cells: short microtubules, which extend directly to the synapse in the pSMAC; and long microtubules, which extend to the rear of the cell (some of which contact the pSMAC and curve past the synapse).[5-7] The polarization of lytic granules toward the MTOC involves dynein-dependent transport along the microtubules in a "minus-end" direction.[8,9] Close to the IS, perforin-containing granules fuse with polarized "exocytic vesicles" carrying effectors, such as Rab27a and Munc13-4. This fusion enables functional maturation of the perforin-containing granules for exocytosis.[10] Lytic granule delivery then occurs in a secretory domain of the IS within the cSMAC. Stinchcombe et al have suggested that, once lytic granules have polarized around the MTOC, secretion is controlled by direct contact between centrosomes and an actin-free area to the plasma membrane (ie, independently of plus-end microtubule motors).[8] However, the consequences of complete inhibition of the plus-end microtubule motors on the CTL's cell cytotoxic activity have never been investigated. Although the critical role of MTOC polarization in inducing granule secretion is now well accepted, it is not clear exactly how lytic granules move along microtubules downstream of the polarized MTOC and dock at the plasma membrane.

The small GTPase Rab27a is an essential effector of the lytic granule exocytic machinery. In humans, Rab27a deficiency is associated with impaired cytotoxic activity, unbalanced expansion, and activation of CD8 T lymphocytes and the uncontrolled macrophage activation that characterizes Griscelli syndrome type 2.[11] The murine homolog of Rab27a deficiency is the natural mutant *ashen.*[12] Microscopic analysis of Rab27a-deficient murine lymphocytes suggests that Rab27a has a role in the terminal transport and/or the docking of cytotoxic granules at the IS.[13] Several effectors of the GTP-bound form of Rab27a have been described and have been grouped into 3 different families on the basis of their constitutive domains: the synaptotagmin-like protein (Slp) family, the Slp-lacking C2 domain (Slac2) family, and the Rab3-binding domain (RBD) family.[14,15] All the effectors have a common N-terminal Rab27-binding Slp-homology domain (SHD). Slp1 and Slp2a are known to be expressed in CTLs and are involved in the secretion of lytic granules.[16,17]

Burkhardt et al reported that the plus-end movement of purified lytic granules was preferentially mediated by the microtubule-dependent motor protein kinesin.[18] In neurons, axonal proteins and cargos are transported by this type of molecular motor, which are essential for anterograde transport. Kinesin-1 (KIF5/KLC, the conventional member of the kinesin superfamily) is a tetrameric protein constituted by 2 heavy chains (KIF5A, KIF5B, or KIF5C) and 2 light chains (KLC1, KLC2, or KLC3) that mediate the plus-end-directed, microtubule-dependent transport of cargos.[19-22] The KIF5A, KIF5C, and KLC1 transcripts are found primarily in neuronal tissues, whereas the KIF5B and KLC2 transcripts are more ubiquitously distributed. KIF5 and KLC have been shown to interact with multiple cargo receptors, adapter, and scaffolding proteins.[23-28] Interestingly, it was recently reported that kinesin-1 regulates the anterograde transport of Slp1/Rab27b-associated vesicles in neurons

via a CRMP2 (collapsin response mediator protein-2) interaction,[29] thus establishing a molecular link between kinesin-1 and the Rab27-Slp machinery.

The precise molecular mechanisms controlling the very late steps in granule delivery to the CTL's IS have not been fully characterized. Polarized granules clustered around the MTOC have just a short distance to travel before they can dock and fuse with the plasma membrane at the IS. Here, we characterized a novel CTL molecular complex formed by specific interactions between Slp3 and Rab27a and recruited by the kinesin-1 motor protein. We also showed that this novel multiprotein complex enables lytic granules to reach the plasma membrane and is thus essential for their release into the IS.

Methods

Plasmid constructs

Human KIF5 DN, KIF5B, KLC1, heptad repeat domain (HPT) KLC1, tetratricopeptide repeat domain (TRP) KLC1, Slp1, and Slp3 sequences were obtained as follows. First, cDNA was prepared from lymphokine-activated killer (Lak) cell mRNA. cDNA was cloned into pCRII-TOPO using the following primers: KIF5A DN (amino acids 402-1028): forward, 5′-CGGAATTCTAACTCATCCATCGTGGTGCGC-3′; reverse, 5′-CGGGATCCTTAGCTGGCTGCTGTCTCTTGGTG-3′; KIF5B: forward, 5′-CGGAATTCTATGGCGGACCTGGCCGAG-3′; reverse, 5′-CGGGTACCTTACACTTGTTTGCCTCCTCC-3′; KLC1: forward, 5′-GCGAATTCGGATGTATGACAACATGTCCACAA-3′; reverse, 5′-GCGGTACCTCAGTTAACCAGCCCGAGC-3′; HPT KLC1: reverse, 5′-CGGGTACCTTATTTGGTAGAATCAGTGTCTTTG-3′; TRP KLC1: forward, 5′-CAAAGACACTGATTCTACCAAATAAGGTACCCG-3′; Slp1: forward, 5′-CGGAATTCAATGCCCCAGAGGGGCCAC-3′; reverse, 5′-GCTCTAGAGGTACCCTACGTCCTGGGGGCCAGG-3′; and Slp3: forward, 5′-CGGAATTCAATGGCCCAAGAAATAGATCTGAG-3′; reverse, 5′-GCTCTAGACCCGGGCTCAGTGCAGGACAAGAGTC-3′. These constructs were then subcloned into pEGFP-C1, mCherry-C1, monomeric DsRed (DsRed), cyan fluorescent protein (CFP)–C1 (Clontech), pcDNA 3.1 His A (Invitrogen), pCMV-HA (Clontech), or 3xFlag (Sigma-Aldrich). Cloning of the human Slp2a-hem isoform has been reported previously.[16] The Slp3 fragments were amplified using the following primers: Slp3-SHD: reverse, 5′-GCGTCGACTTAAGTTGGAAATTTCTTGGC-3′; Slp3-linker: forward, 5′-CGGAATTCAATGCGAGCCAAGAAATTTCCAACT-3′; reverse, 5′-GCTCTAGACCCGGGAGGGGCCACCTGATACTT-3′; and Slp3-2C2: forward, 5′-CGGAATTCAAAGTATCAGGTGGCCCCT-3′. The Slp1 fragment was amplified using the following primers: Slp1-linker: forward, 5′-CGGAATTCACGCTCCCAGCGGCACCAC-3′; reverse, 5′-GCGGTACCTTAGACCTGCACCGCCTCCGC-3′. The Slp2 fragment was amplified using the following primers: Slp2-linker: forward, 5′-GCCTCGAGCTAAGGCAAAAAGGCACAGGGA-3′; reverse, 5′-GCGTCGACTTAGAGCTGGTAACTGCTTTCTG-3′.

Cell culture and transfection

Peripheral blood lymphocytes were grown as described previously.[16] Cytotoxic Lak cells were produced by culturing phytohemagglutinin-induced T-cell blasts with large amounts of IL-2 (1500 IU/mL) for 7 to 25 days. Lak cells were called CTLs all along the manuscript. The YT cell line and L1210-3 target cells were grown in RPMI medium supplemented with 10% FCS. Lak cells and the YT cell line were transfected using the Amaxa nucleofection technique (Amaxa Biosystems), according to the manufacturer's protocols. The stable YT

cell line expressing the green fluorescent protein (GFP)–Slp3 construct was established by successive sorting on GFP^+ cells.

Quantitative PCR

cDNA was prepared from Lak cells, as described in "Cell culture and transfection." Levels of *KIF5A*, *KIF5B*, *KIF5C*, *KLC1*, *KLC2, KLC3*, *SYTL1*, *SYTL2*, *SYTL3*, *SYTL4*, *SYTL5*, and *RAB27A* transcripts were determined by quantitative PCR using: TaqMan Gene expression Master Mix (Applied Biosystems), primer (*KIF5A*:Hs00192120_m1, *KIF5B*:Hs01037194_m1, *KIF5C:* Hs00189672_m1, *KLC1*:Hs00194316_m1, *KLC2:* Hs03988192_m1, *KLC3:* Hs00377104_m1, *SYTL1*:Hs01070946_m1, *SYTL2* Hs00262977_m1, *SYTL3*:Hs00292065_m1, *SYTL4*:Hs00299039_m1, *SYTL5*:Hs00371091_m1, *RAB27A*:Hs00608302_m1, and *ACTB*:Hs99999903_m1; Applied Biosystems), and cDNA. Each sample was amplified in triplicate on a real-time PCR instrument (an ABI 7900 cycler) and analyzed using Sequence Detection Systems software (Version 2.2.2, Applied Biosystems). The relative mRNA levels were quantified via the comparative C_t method and normalized against the average values of *ACTB* as endogenous control. *KIF5A*, *KIF5B*, *KIF5C*, *KLC1*, *KLC2*, and *KLC3* transcript levels were then expressed as a proportion of the mean value of *KLC1. SYTL1, SYTL2*, *SYTL3*, *SYTL4*, and *SYTL5* values were expressed as a proportion of the mean value of *RAB27A*.

Mass spectrometry and protein identification

Mass spectrometry and protein identification were performed as described previously.[16]

Immunoprecipitation

Constructs were coexpressed in 293T cells. One day after transfection, cells were lysed in lysis buffer (20mM Tris, pH 7.4, 150mM NaCl, 0.1% NP40) supplemented with 1 EDTA-free protease inhibitor cocktail tablet (Roche Diagnostics) and phosphatase inhibitors (Sigma-Aldrich). Immunoprecipitation was performed with FLAG M2 affinity gel (Sigma-Aldrich), anti-GFP antibody (Roche Diagnostics), or protein G-agarose beads (Sigma-Aldrich). Anti-M2 (Sigma-Aldrich), anti-GFP full-length (Roche Diagnostics), anti-HA (Roche Diagnostics), and anti-KLC1 (Millipore) antibodies were used to develop the Western blots.

Conjugate formation

L1210-3 target cells were mixed 1:1 with transfected Lak cells in the presence of anti-CD3 (7.5 μg/mL, OKT3, Ortoclone) and incubated for 10 minutes at 37°C. The cells were then plated on glass coverslips coated with poly–L-lysine (Sigma-Aldrich) and incubated for 20 minutes at 37°C.

Immunofluorescence microscopy

The following antibodies and labels were used: purified mouse monoclonal anti–human perforin (deltaG9; BD Biosciences PharMingen), AlexaFluor-488–conjugated anti-perforin (BioLegend), anti–α-tubulin (Rockland), and AlexaFluor-555–conjugated goat anti–mouse IgG F(ab')2 secondary antibodies (Invitrogen).

Confocal fluorescence images were acquired with a LSM 700 microscope (Carl Zeiss). Image datasets were processed with Zeiss LSM Image Browser or Adobe Photoshop (Version CS) software. Colocalization studies were analyzed with the Imaris Version 6.4.2. Colocalization Module (BitPlane AG).

siRNA

Specific duplex siRNA targeting KIF5B (5′-AAACCGAGTTCCCTATCTAAA-3′) was generated as described by Wiesner et al.[30] Control siRNA was purchase from Santa Cruz Biotechnology. The degranulation essay was performed 72 hours after transfection. Statistical analysis (using a Mann-Whitney test) was performed with Prism Version 4 software. The threshold for statistical significance was set to $P < .05$.

The total internal reflection fluorescence assay

The total internal reflection fluorescence (TIRF) assay was performed on the transfected CTLs as described in "Cell culture and transfection." Anti-CD3 antibody (7.5 μg/mL, OKT3, Ortoclone)–coated glass coverslips were used to stimulate 3×10^5 transfected Lak cells per coverslip. Cells were incubated for 20 minutes at 37°C in 5% CO_2 and then fixed in 3.7% paraformaldehyde. Fluorescence data were acquired with the Nikon Eclipse Ti-E TIRF imaging system. Images were recorded with the Nikon Ropper scientific QuanTEM 512 SC camera and analyzed with NIS-Elements AR software (Version 3.1). Image sets were processed with ImageJ Version 1.43 software. Statistical analysis using a Mann-Whitney test was performed with Prism Version 4 (GraphPad software). The threshold for statistical significance was set to $P < .0001$.

The degranulation assay

Lak cell degranulation was measured by monitoring the expression of the lysosomal marker proteins CD107a and CD107b. An anti-CD3 antibody (7.5 μg/mL, OKT3, Ortoclone) coating in a 96-well plate was used to stimulate 3×10^5 transfected Lak cells/well in the presence of anti-CD107a–FITC and anti-CD107b–FITC. Cells were incubated for 3 hours at 37°C in 5% CO_2. Thereafter, cells were harvested, washed once with PBS-0.02% azide, stained with anti–CD3-allophycocyanin (APC) and anti-CD8–PE (BD Biosciences), and analyzed by flow cytometry. Data were analyzed with FlowJo Version 8.8.4 software (TreeStar). The CFP empty vector was used to define the CFP^+ gate in all settings, as shown in supplemental Figure 1 (available on the *Blood* Web site; see the Supplemental Materials link at the top of the online article). Values are based on 3 representative, independent experiments in which each condition was tested in duplicate.

Results

Expression of kinesin-1 (KIF5B/KLC1) and Slp family members in CTLs

In neurons, kinesin-1 has been recently shown to regulate the anterograde transport of Rab27b-Slp1–associated vesicles on microtubules.[29] We thus looked at whether kinesin-1 (in association with a Rab27a-Slp complex) similarly regulates cytotoxic function in CTLs via the transport of Rab27a-Slp–associated vesicles. To address this question, we first analyzed the expression of the different isoforms of the kinesin heavy chain (KHC) and kinesin light chain (KLC) in CTLs. Quantitative RT-PCR for the 3 KHC (*KIF5A, KIF5B*, and *KIF5C*) and the 3 KLC mRNA (*KLC1*, *KLC2*, and *KLC3*) identified KIF5B and KLC1 as the main KHC and KLC isoforms present in CTLs, respectively (Figure 1A). A small amount of KLC2 was also detected.

In a previous study of CTLs, we had identified a hematopoietic form of Slp2a that was able to interact with the active form of Rab27a.[16] Using an updated database to reanalyze previously generated mass spectrometry data on proteins coimmunoprecipitated with Rab27a, we in addition identified an Slp3-specific peptide sequence (Figure 1B). To confirm that Slp3 is able to interact with Rab27a, we coexpressed Slp3 with Rab27a fused to a Flag tag in 293T cells. As shown in Figure 1C, Flag immunoprecipitation revealed a strong interaction between Slp3 and Rab27a, in agreement with a previous report by Kuroda et al.[14]

To investigate the Slp3's subcellular localization, we transiently expressed a full-length GFP-tagged Slp3 in nonconjugated CTLs. Slp3 was found to be present in both cytosolic and vesicular structures (Figure 1D top panel). To determine whether Slp3 targets the same granules as Rab27a, we engineered CTLs to coexpress GFP-Slp3 and the monomeric fluorescence protein red fused to Rab27a (DsRed-Rab27a). A strong overlap of the 2 fluorescence signals was observed (Slp3/Rab27a, 96.3% ± 3.2% overlap; Figure 1D bottom panel). These data indicate that the Slp3 protein is expressed in CTLs and interacts with Rab27a on vesicular structures. It has also been reported that CTLs express Slp1 protein.[17] To screen more systematically for the expression of the 5 known members of the Slp family in CTLs, we implemented a quantitative PCR approach. Slp3 and (to a lesser extent) Slp1 were the mostly highly expressed Slp transcripts in CTLs (Figure 1E). Slp2a expression was barely detectable and was 10-fold less intense than Slp3 transcript expression. Rab27a's higher affinity for Slp2a than for Slp3 (as previously reported[31]) could explain why Slp2a was first characterized as Rab27a's main protein partner in CTLs. However, a unique role of Slp2a in lytic granule exocytosis could not be demonstrated.[16,17] We did not detect Slp4/granuphilin and Slp5 transcripts (data not shown). Thus, 3 members of the Slp families (Slp1, Slp2a, and Slp3) are expressed in CTLs and are potential candidates for the mediation of a kinesin-1 function in these cells. Together with the KIF5B/KLC1 isoforms of kinesin-1, Slp1 and Slp3 are more strongly expressed than Slp2a in CTLs.

Slp3 binds to the kinesin-1 motor through interaction with KLC1

We then established whether KLC1 (which is known to interact with several cargo receptors and adapter proteins[25-28]) can interact with members of the Slp family. To this end, Slp1-, Slp2-, or Slp3-Flag–tagged constructs were expressed with GFP-KLC1 in 293T cells and examined in immunoprecipitation assays. As shown in Figure 2A, an interaction between KLC1 and Slp3 was observed, whereas no interaction was detected with Slp1 or Slp2a. In contrast, no interaction between KIF5B and any of the 3 Slp proteins could be observed (supplemental Figure 2). The members of the Slp family contain an N-terminal SHD, a linker region, and a C-terminal tandem C2 domain.[14] To determine which region of Slp3 is involved in KLC1 binding, we generated 3 GFP-tagged constructs of Slp3 containing an SHD linker or C2 domain. (Figure 2B). Each Slp3 construct was coexpressed with HA-KLC1 in 293T cells and examined in immunoprecipitation assays. The Slp3-SHD and -tandem C2 domains (2C2) did not associate with KLC1. In contrast, the linker domain of Slp3 was able to bind KLC1 (Figure 2B). To identify the region of KLC1 involved in Slp3 interaction, the N-terminal HPT and the C-terminal TRP of KLC1 were generated and used in binding experiments. Slp3 was only able to interact with the TRP domain of KLC1 (Figure 2C). Because an anti-endogenous Slp3 antibody was not available, we generated a stable YT cell line expressing a GFP-Slp3 construct. When the YT cell lysates were immunoprecipitated with anti-KLC1 antibody, GFP-Slp3 was found to be associated with the endogenous KLC1 (Figure 2D). These results demonstrate that the Slp3 linker region interacts with the TRP domain of the KLC1 subunit of kinesin-1. Slp3 appears to be the only isoform capable of interacting directly with kinesin-1. This contrasts with the situation for Slp1, which interacts with kinesin-1 via the recruitment of CRMP2.[29]

Kinesin-1 regulates a late step in lytic granule exocytosis

In a CTL conjugated with a target cell, the microtubule minus-end–directed motor protein dynein is sufficient to drive lytic granule transport toward the MTOC, which is polarized toward the IS.[8,9] Identification of the Slp3-KLC1 complex in CTLs prompted us to look at whether the microtubule plus-end molecular motor protein kinesin-1 could be involved in lytic granule release. We first determined KIF5B's subcellular localization. To this end, we expressed a GFP-KIF5B fusion protein in CTLs. The GFP-KIF5B distributed along microtubules and around the MTOC (tubulin/KIF5B, 93.2% ± 6.7% overlap; Figure 3 top

panel). We next investigated the localization of a truncated, dominant-negative mutant of KIF5A (KIF5 DN) lacking the kinesin ATPase motor domain of the KHC.[25,32] The KIF5 DN protein was concentrated around the MTOC, with only low levels in the cytosol (tubulin/KIF5 DN, 72.8% ± 1.5% overlap; Figure 3A bottom panel). The KIF5 constructs' localization at the MTOC may be the result of recruitment of kinesin-1 to the pericentriolar matrix protein via Rootletin, known to interact directly with the KLC1 subunit.[33,34]

We next investigated the role of kinesin-1 in lytic granule secretion by testing for the presence of CD107a/b at the CTL plasma membrane after TCR stimulation in the presence of KIF5 DN. KIF5B and KIF5 DN were fused to a CFP that enabled detection in the transfected CTL population. Expression of the KIF5B construct did not modify CTL degranulation compared with nontransfected CTLs or CFP-transfected CTLs (Figure 3B and supplemental Figures 1 and 4). In contrast, CTL degranulation was severely impaired in cells expressing KIF5 DN (Figure 3B; supplemental Figure 4), even though the lytic granules were normally polarized toward the target cell (Figure 3C). To further demonstrate the role of kinesin-1 in lytic granule exocytosis, we used siRNA[30] to knockdown KIF5B in CTL. The efficacy of siRNA targeting KIF5B was checked in the 293T cell line; as shown in supplemental Figure 3, the amount of endogenous KIF5B fell by 80%. Next, CTLs were cotransfected with siRNA and CFP to assess the transfectants' ability to degranulate. As shown in Figure 3D, reduced KIF5B expression was associated with a significant decrease in the CTLs' ability to degranulate. These data show that expression of a dominant-negative form of KIF5 impairs lytic granule secretion but does not prevent granules from polarizing toward the MTOC. Furthermore, silencing of KIF5B impairs lytic granule secretion. Kinesin-1 is thus an essential effector of lytic granule exocytosis downstream of granule and MTOC polarization toward the CTL-target cell contact zone.

Antagonistic roles of Slp1, Slp2a, and Slp3 in lytic granule exocytosis

We then assessed the role of each of the expressed Slp members in lytic granule secretion in CTLs by performing a degranulation assay in CTLs overexpressing wt-Slp1–, wt-Slp2a–, or wt-Slp3– CFP constructs. CTLs overexpressing wt-Slp2a were found to degranulate normally (Figure 4A; supplemental Figure 4), whereas degranulation was totally abrogated in CTLs overexpressing Slp1 or Slp3 (Figure 4A; supplemental Figure 4). As previously observed in cells expressing KIF5 DN, polarization of Slp3-associated vesicles and perforin-containing granules toward the conjugated target cell was normal (Figure 4B). As shown in Figure 4B, perforin-containing granules colocalized with Slp3 near the cell-cell contact site (overlap: 71.9% ± 12%). In contrast, Slp1 was mainly distributed at the CTL's plasma membrane, as previously reported.[17] This functional inhibition may result from the overexpression of a single component affecting the balance between endogenous complexes. We thus looked at whether lytic granule exocytosis could be restored by increasing the Rab27a/Slp ratio. As shown in Figure 4C, coexpression of an unlabeled Rab27a construct and CFP-Slp3 rescued the degranulation defect associated with Slp3 overexpression (supplemental Figure 4). In contrast, coexpression of Rab27a and CFP-Slp1 did not significantly rescue the degranulation defect associated with Slp1 overexpression (Figure 4C; supplemental Figure 4). Taken as a whole, these results suggest that: (1) the Rab27a/Slp3 complex has a role in lytic granule secretion at the IS; and (2) Slp1 could behave differently from Slp3 in CTLs by acting as a membrane-bound negative regulator of granule exocytosis.

The critical role of the Slp3 linker region in lytic granule release

After our identification of the linker as the region of Slp3 that interacts with KLC1, we decided to look at whether overexpression of this linker fragment could similarly affect CTL degranulation. As expected, cells overexpressing a CFP-Slp3-linker construct were no

longer able to degranulate (Figure 5A; supplemental Figure 4). In contrast, overexpression of CFP-Slp1– or -Slp2–linker constructs (which are not able to interact with KLC1) did not significantly impair degranulation (Figure 5A; supplemental Figure 4). The Slp3-linker's subcellular localization was investigated by transiently expressing a GFP-tagged version in CTLs. We observed strong overlap between the Slp3-linker on one hand and (1) MTOC labeled with anti-tubulin (Figure 5B) and (2) transiently expressed KLC1 (Figure 5C) on the other hand (tubulin/Slp3, 93.7% ± 5% overlap; Slp3/KLC1, 73.4% ± 1.8% overlap). This observation further supports a role for Slp3 in the recruitment of Rab27a-associated structures to the kinesin-1 motor. We then determined whether the polarization of perforin-containing granules toward the target cell was affected in Slp3-linker–transfected CTLs. Once again, the impairment in granule secretion (resulting from the Slp3-linker dominant effect) was not associated with defective lytic granule polarization (Figure 5D). Taken as a whole, these results further emphasize the functional role of a Slp3-KLC1 interaction in lytic granule exocytosis downstream of the MTOC-driven polarization of granules toward the IS.

Kinesin-1 regulates vesicle transport to the IS

To characterize kinesin-1's functional role in the CTL's exocytic lytic machinery, we further investigated the effect of the dominant-negative construct of KIF5 on Rab27a/Slp3-associated compartment. Cytotoxic T lymphocytes were transfected with KIF5B or KIF5 DN fused to GFP, Slp3 fused to DsRed and unlabeled Rab27a (Figure 6A, Slp3/KIF5B, 70.3% ± 8.7% overlap; Slp3/KIF5 DN, 56.6% ± 3.6% overlap). Conjugate cell formation indeed led to the polarization of both labeled proteins. However, in the presence of KIF5 DN, the Slp3-associated compartment was unable to reach and dock at the IS (Figure 6A bottom panel). In addition, degranulation of the KIF5 DN-transfected cells was profoundly impaired, whereas cells expressing KIF5B were able to degranulate normally (Figure 6B; supplemental Figure 4). To investigate the distance between the Rab27a/Slp3 compartment and the IS in more detail, we performed TIRF imaging of transfected CTLs on anti-CD3 antibody-coated glass coverslips. The CTLs were transfected with KIF5B or KIF5 DN fused to DsRed, GFP-Slp3, and GFP-Rab27a. As shown in Figure 6C, the number of Rab27a/Slp3 vesicles detected by TIRF imaging was significantly lower in KIF5 DN-expressing cells than in KIF5B-expressing cells ($P < .0001$). These results indicate, that in the absence of functional kinesin-1, polarized Rab27a/Slp3-associated compartment is unable to reach the plasma membrane and thus the IS.

Discussion

Cytotoxic granule exocytosis by CTLs at the IS is a critical and highly regulated process through which infected or transformed cells are eliminated. Secretion occurs after the cytotoxic granules have clustered around the MTOC, become polarized, and are transported to the plasma membrane. Previous work has shown that the minus-end–mediated transport of cytotoxic granules to the MTOC is dynein-dependent.[8,9] In the present study, we provide evidence of an additional, downstream, plus-end kinesin-dependent transport step that enables polarized cytotoxic granules to reach the membrane and release their contents at the IS (Figure 7). This step includes Slp3 recruitment by granule-associated Rab27a and interaction with the C-terminal of the KLC1. Taken as a whole, our data enabled us to identify a new transport step and describe a molecular complex that is essential for cytotoxic function in CTLs.

KIF5B and KLC1 turned out to be the main isoforms of the kinesin-1 heavy chain and light chain, respectively, expressed in CTLs. Furthermore, Slp3 was identified as a new Rab27a effector expressed in CTLs and served as a cargo receptor to link Rab27-associated granules to kinesin-1. KIF5B, the ubiquitous heavy chain, also expressed in non-neuronal cells, mediates the anterograde movement of associated vesicles via its head domain. The KIF5B

tail domain and its associated light chains are involved in vesicular cargo binding.[19-22,35] We found that the light chain KLC1 was the only chain capable of mediating the kinesin-1–Slp3-vesicular cargo interaction in CTLs. KLC1's C-terminal TRP binds directly to Slp3 through the linker region, for which functional interactions had not previously been identified. Only a few KLC cargo receptors, such as the Trk neurotrophin receptors in neurons,[29] have been reported. Interestingly, the kinesin-1–mediated anterograde movement of TrkB-containing vesicles to the axon terminus also depends on a Rab27-Slp transport complex that is reminiscent of the one identified here in CTLs. Indeed, Slp1 in neurons and Slp3 in CTLs cells bind to an active, membrane-associated form of Rab27a through their SHD domain. The Slp1 and Slp3 proteins are recruited by kinesin-1 via the TRP of KLC1. In neurons, Slp1 interacts indirectly with TRP-KLC1 by recruiting the CRMP2. In contrast, the Slp3 linker region directly binds to TPR-KLC1 in CTLs. Although CRMP2 is expressed in lymphocytes, it is not required for the Slp3–kinesin-1 interaction. Given that Slp1 is also expressed in CTLs, we cannot rule out the possibility that (in addition to the Rab27a/Slp3/KLC1 complex identified here) a Rab27a/Slp1/CRMP2/KLC1 complex may also form and be involved in vesicle transport and exocytosis. Previous studies have attributed Slp proteins with a key role in vesicle docking. Our data support a broader role of Slp proteins functioning as molecular adapters and cargo vesicle receptors.

Kinesin-1's involvement in lytic granule secretion was demonstrated by inhibiting the protein's transport function via (1) the expression of a dominant-negative form of KIF5, (2) KIF5B silencing, and (3) overexpression of the cognate Slp3 linker region. In all these settings, the functional inhibition of kinesin-1 did not modify the polarization of the MTOC and the lytic granules toward the IS. However, kinesin-1 function was required for the transport of cytotoxic granules from the MTOC to the plasma membrane. In CTLs lacking functional kinesin-1, the Rab27a/Slp3-associated granules do not reach the plasma membrane; thus, the granule contents are not delivered to the IS. These data fit with the known dynein motor requirement for the movement of cytotoxic granules to the MTOC.[8,9] We now propose that the transport of granules from the MTOC to the secretion site requires kinesin-1. In a very similar manner, kinesin-1 has been shown to be involved in regulation of the last step of secretion in various cell types. In macrophages, this molecular motor is responsible for the secretion of recycling endosomes into the phagocytic cup.[36] In pancreatic β-cells, kinesin-1 controls insulin secretion in response to a glucose challenge.[37]

Of the 3 different Slp proteins that were expressed in CTLs and able to bind active Rab27a, Slp3 was the only one to interact directly with kinesin-1. Because Slp3 appears to be essential for connecting Rab27a-associated granules to the kinesin machinery, this adaptor function probably accounts for the inhibition of granule exocytosis observed when Slp3 is overexpressed; the greater the amount of Slp3, the lower the likelihood of simultaneously binding Rab27a and kinesin-1. Accordingly, coexpression of Rab27a and Slp3 restored the function of the tripartite complex. We were surprised to find that the inhibition of granule secretion by Slp1 overexpression in CTLs was not rescued by increasing the levels of Rab27a (in contrast to what was observed for Slp3). This finding suggests that the Rab27a-Slp1 complex and the Rab27a-Slp3 complex do not regulate lytic granule secretion in the same way. This hypothesis is supported by our observation of a predominantly plasma membrane localization of Slp1 (in agreement with the report by Holt et al[17]). We also wondered whether Slp2a has a unique function in lytic granule secretion or whether Slp proteins are functionally redundant. Impaired lytic granule-dependent cytotoxicity was not seen in Slp1- and Slp2-knockout mice.[17] To the best of our knowledge, Slp3-knockout mice have not been reported. However, our attempt to silence Slp3 expression in human CTLs failed to significantly impair lytic granule secretion (data not shown). It may be that the Slp3 silencing in our experiment was not intense enough to affect what is a very efficient function in CTLs. Nevertheless, these data do not rule out the possibility that in vivo, a sequential

interaction of Rab27a with different Slp effectors may be required to closely regulate the formation of a pool of mature cytotoxic granules and then the secretion of a few mature granules at a precise site within the IS. Further work will be required to better determine the role and importance of each Slp-Rab27a effector in lytic granule secretion.

We found that inhibition of the kinesin-1 function in CTLs impairs both the terminal transport of Rab27a-associated vesicles and the exocytosis of cytotoxic granules. This strongly suggests that both organelles are functionally linked. We previously established that, in CTLs recognizing a target cell, lytic granules undergo a final maturation step via the fusion of perforin-containing granules with an endosomal compartment bearing Rab27a, Munc13-4, and Slp exocytic effectors.[10] This late maturation step may occur once both types of organelle have been brought close to the IS with the MTOC, after kinesin-1 has taken over from dynein in the granule transport process. Thus, our findings support a role for the Rab27a-Slp3–kinesin-1 complex in the transport of cytotoxic granules that have been functionally licensed by acquisition of the exocytic machinery. We cannot rule out a role of the Rab27a-Slps-kinesin-1 complex in the granule maturation process (ie, fusion between lytic granules and “exocytic vesicles”). Determining the molecular mechanisms that complete the maturation of cytotoxic granules will be an important further step.

Our observation of the decisive role of kinesin-1 in the area of the cell in which cytotoxic granules undergo late maturation provides additional evidence to suggest that, after granule recruitment to the IS, exocytosis is tightly regulated at critical checkpoints close to the plasma membrane. By analogy with the neural synapse, this limited area can be viewed as a presynaptic “active zone” of the IS and is built by the transient reorganization and redistribution of a network of proteins. This network coordinates the signaling, trafficking, docking, priming, and fusion events that culminate in lytic granule secretion and target cell killing. In the “active zone” of the IS, kinesin-1 transports cytotoxic granules to the plus-ends of microtubules inserted into the reorganized F-actin network. An actin motor protein could potentially take over from kinesin-1 and transport the cytotoxic granules to the secretion site. In NK cells, myosin IIA has been shown to facilitate lytic granule transit through the F-actin–rich area of the IS.[38] Interestingly, recent studies have underlined the importance of the strength of TCR stimulation in dictating the path of lytic granules to specific locations within the IS. Weak TCR stimulation deviates lytic granules to the pSMAC before they reach the secretory domain in the cSMAC, whereas strong TCR stimulation leads to direct recruitment of the granules to the cSMAC.[39,40] Depending on the signaling strength, kinesin-1 and myosin IIA may play distinct roles in direct lytic granule transport to the secretion site.

Here, we identified a novel function for kinesin-1 and its Rab27a-Slp3–associated molecular complex in CTL activity. In addition to the dynein-dependent movement of cytotoxic granules toward the MTOC, lytic granules undergo plus-ended microtubule motility via a kinesin transport complex that transits granules to the IS. Thus, in place of a direct delivery of the cytotoxic granules to the plasma membrane by centrosome as previously proposed,[8] our findings favor a kinesin-dependent granule delivery at the final step of secretion. This newly identified transport step constitutes a further element of the mechanism that regulates the polarized secretion of cytotoxic granules in space and time.

Acknowledgments

The authors thank Nathalie Prince for expert technical assistance and Marjorie Cote, Agathe Burgess, Roxane Lemoine, and Fernando Sepulveda for discussions and assistance.

This work was supported by Inserm, Agence Nationale de la Recherche (ANR/GENOPAT), and the European Research Council. N.T.N. was supported by Association pour la Recherche sur le Cancer.

References

1. Voskoboinik I, Smyth MJ, Trapani JA. Perforin-mediated target-cell death and immune homeostasis. Nat Rev Immunol. 2006; 6(12):940–952. [PubMed: 17124515]
2. de Saint Basile G, Menasche G, Fischer A. Molecular mechanisms of biogenesis and exocytosis of cytotoxic granules. Nat Rev Immunol. 2010; 10(8):568–579. [PubMed: 20634814]
3. Jenkins MR, Griffiths GM. The synapse and cytolytic machinery of cytotoxic T cells. Curr Opin Immunol. 2010; 22(3):308–313. [PubMed: 20226643]
4. Stinchcombe JC, Bossi G, Booth S, Griffiths GM. The immunological synapse of CTL contains a secretory domain and membrane bridges. Immunity. 2001; 15(5):751–761. [PubMed: 11728337]
5. Kuhn JR, Poenie M. Dynamic polarization of the microtubule cytoskeleton during CTL-mediated killing. Immunity. 2002; 16(1):111–121. [PubMed: 11825570]
6. Poenie M, Kuhn J, Combs J. Real-time visualization of the cytoskeleton and effector functions in T cells. Curr Opin Immunol. 2004; 16(4):428–438. [PubMed: 15245735]
7. Combs J, Kim SJ, Tan S, et al. Recruitment of dynein to the Jurkat immunological synapse. Proc Natl Acad Sci U S A. 2006; 103(40):14883–14888. [PubMed: 16990435]
8. Stinchcombe JC, Majorovits E, Bossi G, Fuller S, Griffiths GM. Centrosome polarization delivers secretory granules to the immunological synapse. Nature. 2006; 443(7110):462–465. [PubMed: 17006514]
9. Mentlik AN, Sanborn KB, Holzbaur EL, Orange JS. Rapid lytic granule convergence to the MTOC in natural killer cells is dependent on dynein but not cytolytic commitment. Mol Biol Cell. 2010; 21(13):2241–2256. [PubMed: 20444980]
10. Menager MM, Menasche G, Romao M, et al. Secretory cytotoxic granule maturation and exocytosis require the effector protein hMunc13-4. Nat Immunol. 2007; 8(3):257–267. [PubMed: 17237785]
11. Menasche G, Pastural E, Feldmann J, et al. Mutations in RAB27A cause Griscelli syndrome associated with haemophagocytic syndrome. Nat Genet. 2000; 25(2):173–176. [PubMed: 10835631]
12. Wilson SM, Yip R, Swing DA, et al. A mutation in Rab27a causes the vesicle transport defects observed in ashen mice. Proc Natl Acad Sci U S A. 2000; 97(14):7933–7938. [PubMed: 10859366]
13. Stinchcombe JC, Barral DC, Mules EH, et al. Rab27a is required for regulated secretion in cytotoxic T lymphocytes. J Cell Biol. 2001; 152(4):825–834. [PubMed: 11266472]
14. Kuroda TS, Fukuda M, Ariga H, Mikoshiba K. The Slp homology domain of synaptotagmin-like proteins 1-4 and Slac2 functions as a novel Rab27A binding domain. J Biol Chem. 2002; 277(11): 9212–9218. [PubMed: 11773082]
15. Wang J, Takeuchi T, Yokota H, Izumi T. Novel rabphilin-3-like protein associates with insulin-containing granules in pancreatic beta cells. J Biol Chem. 1999; 274(40):28542–28548. [PubMed: 10497219]
16. Menasche G, Menager MM, Lefebvre JM, et al. A newly identified isoform of Slp2a associates with Rab27a in cytotoxic T cells and participates to cytotoxic granule secretion. Blood. 2008; 112(13):5052–5062. [PubMed: 18812475]
17. Holt O, Kanno E, Bossi G, et al. Slp1 and Slp2-a localize to the plasma membrane of CTL and contribute to secretion from the immunological synapse. Traffic. 2008; 9(4):446–457. [PubMed: 18266782]
18. Burkhardt JK, McIlvain JM Jr, Sheetz MP, Argon Y. Lytic granules from cytotoxic T cells exhibit kinesin-dependent motility on microtubules in vitro. J Cell Sci. 1993; 104(1):151–162. [PubMed: 8449993]
19. Hirokawa N. Kinesin and dynein superfamily proteins and the mechanism of organelle transport. Science. 1998; 279(5350):519–526. [PubMed: 9438838]
20. Xia C, Rahman A, Yang Z, Goldstein LS. Chromosomal localization reveals three kinesin heavy chain genes in mouse. Genomics. 1998; 52(2):209–213. [PubMed: 9782088]

21. Rahman A, Friedman DS, Goldstein LS. Two kinesin light chain genes in mice: identification and characterization of the encoded proteins. J Biol Chem. 1998; 273(25):15395–15403. [PubMed: 9624122]
22. Morton AM, Cunningham AL, Diefenbach RJ. Kinesin-1 plays a role in transport of SNAP-25 to the plasma membrane. Biochem Biophys Res Commun. 2010; 391(1):388–393. [PubMed: 19913510]
23. Su Q, Cai Q, Gerwin C, Smith CL, Sheng ZH. Syntabulin is a microtubule-associated protein implicated in syntaxin transport in neurons. Nat Cell Biol. 2004; 6(10):941–953. [PubMed: 15459722]
24. Ferreira A, Niclas J, Vale RD, Banker G, Kosik KS. Suppression of kinesin expression in cultured hippocampal neurons using antisense oligonucleotides. J Cell Biol. 1992; 117(3):595–606. [PubMed: 1533397]
25. Kimura T, Watanabe H, Iwamatsu A, Kaibuchi K. Tubulin and CRMP-2 complex is transported via Kinesin-1. J Neurochem. 2005; 93(6):1371–1382. [PubMed: 15935053]
26. Konecna A, Frischknecht R, Kinter J, et al. Calsyntenin-1 docks vesicular cargo to kinesin-1. Mol Biol Cell. 2006; 17(8):3651–3663. [PubMed: 16760430]
27. Kamal A, Stokin GB, Yang Z, Xia CH, Goldstein LS. Axonal transport of amyloid precursor protein is mediated by direct binding to the kinesin light chain subunit of kinesin-I. Neuron. 2000; 28(2):449–459. [PubMed: 11144355]
28. Verhey KJ, Meyer D, Deehan R, et al. Cargo of kinesin identified as JIP scaffolding proteins and associated signaling molecules. J Cell Biol. 2001; 152(5):959–970. [PubMed: 11238452]
29. Arimura N, Kimura T, Nakamuta S, et al. Antero-grade transport of TrkB in axons is mediated by direct interaction with Slp1 and Rab27. Dev Cell. 2009; 16(5):675–686. [PubMed: 19460344]
30. Wiesner C, Faix J, Himmel M, Bentzien F, Linder S. KIF5B and KIF3A/KIF3B kinesins drive MT1-MMP surface exposure, CD44 shedding, and extracellular matrix degradation in primary macrophages. Blood. 2010; 116(9):1559–1569. [PubMed: 20505159]
31. Schneider M, Lu W, Neumann S, et al. Molecular mechanisms of centrosome and cytoskeleton anchorage at the nuclear envelope. Cell Mol Life Sci. 2010; 68(9):1593–1610. [PubMed: 20922455]
32. Fukuda M. Distinct Rab27A binding affinities of Slp2-a and Slac2-a/melanophilin: Hierarchy of Rab27A effectors. Biochem Biophys Res Commun. 2006; 343(2):666–674. [PubMed: 16554019]
33. Kawano Y, Yoshimura T, Tsuboi D, et al. CRMP-2 is involved in kinesin-1-dependent transport of the Sra-1/WAVE1 complex and axon formation. Mol Cell Biol. 2005; 25(22):9920–9935. [PubMed: 16260607]
34. Yang J, Li T. The ciliary rootlet interacts with kinesin light chains and may provide a scaffold for kinesin-1 vesicular cargos. Exp Cell Res. 2005; 309(2):379–389. [PubMed: 16018997]
35. Xu M, Gu Y, Barry J, Gu C. Kinesin I transports tetramerized Kv3 channels through the axon initial segment via direct binding. J Neurosci. 2010; 30(47):15987–16001. [PubMed: 21106837]
36. Silver KE, Harrison RE. Kinesin 5B is necessary for delivery of membrane and receptors during FcgammaR-mediated phagocytosis. J Immunol. 2010; 186(2):816–825. [PubMed: 21149599]
37. Cui J, Wang Z, Cheng Q, et al. Targeted inactivation of kinesin-1 in pancreatic beta cells in vivo leads to insulin secretory deficiency. Diabetes. 2011; 60(1):320–330. [PubMed: 20870970]
38. Andzelm MM, Chen X, Krzewski K, Orange JS, Strominger JL. Myosin IIA is required for cytolytic granule exocytosis in human NK cells. J Exp Med. 2007; 204(10):2285–2291. [PubMed: 17875677]
39. Beal AM, Anikeeva N, Varma R, et al. Kinetics of early T cell receptor signaling regulate the pathway of lytic granule delivery to the secretory domain. Immunity. 2009; 31(4):632–642. [PubMed: 19833088]
40. Jenkins MR, Tsun A, Stinchcombe JC, Griffiths GM. The strength of T cell receptor signal controls the polarization of cytotoxic machinery to the immunological synapse. Immunity. 2009; 31(4):621–631. [PubMed: 19833087]

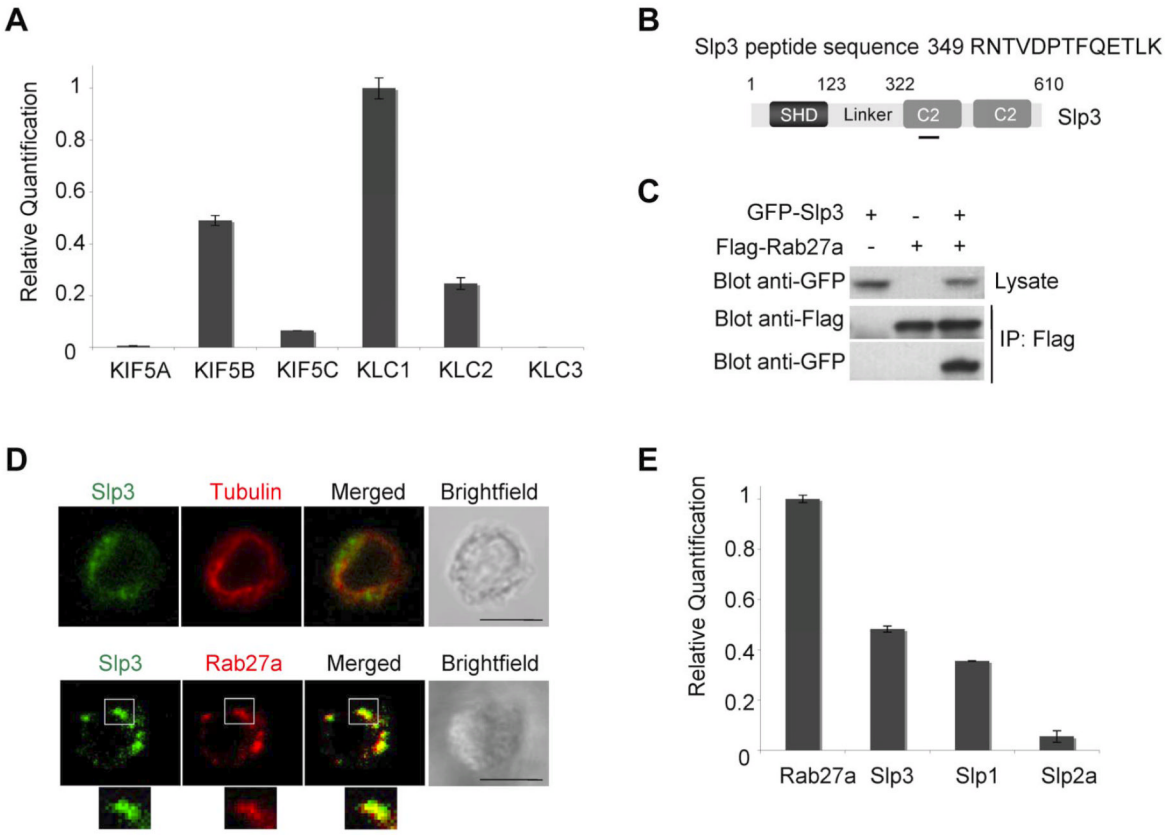

Figure 1. Kinesin-1 (KIF5B/KLC1), Slp1, Slp2a, and Slp3 expression in CTLs

(A) Relative quantification of KIF5A, KIF5B, KIF5C, KLC1, KLC2, and KLC3 transcripts in a real-time PCR with CTL mRNA. Transcript levels for each sample were expressed as a proportion of the mean value for KLC1. The data are representative of 2 independent experiments performed in duplicate. (B) A schematic representation of the Slp3 domains used to localize the peptide identified by mass spectrometry. The peptide sequence is shown. (C) Flag-Rab27a and GFP-Slp3 were coexpressed into 293T cells. Cell lysates were immunoprecipitated with anti-Flag antibody (M2 beads) and then separated by SDS-PAGE. Coprecipitated Rab27a and Slp3 were immunoblotted with anti-Flag and anti-GFP antibodies. The blots represent 3 independent experiments. (D) Top panel: confocal microscopy of CTLs transfected with GFP-Slp3. Cells were then fixed, permeabilized, and stained with anti-tubulin (in red). Bottom panel: confocal microscopy of CTLs transfected with GFP-Slp3 and DsRed-Rab27a. The lower insets represent an enlarged image. Scale bars represent 5 μm. All images of single cells were representative of > 60 cells observed over at least 4 independent experiments performed in duplicate. (E) Relative quantification of Rab27a, Slp1, Slp2, and Slp3 transcripts was performed by real-time PCR of CTL mRNA. Transcript levels for each sample were expressed as a proportion of the mean value of Rab27a. The data are representative of 2 independent experiments performed in duplicate.

Europe PMC Funders Author Manuscripts

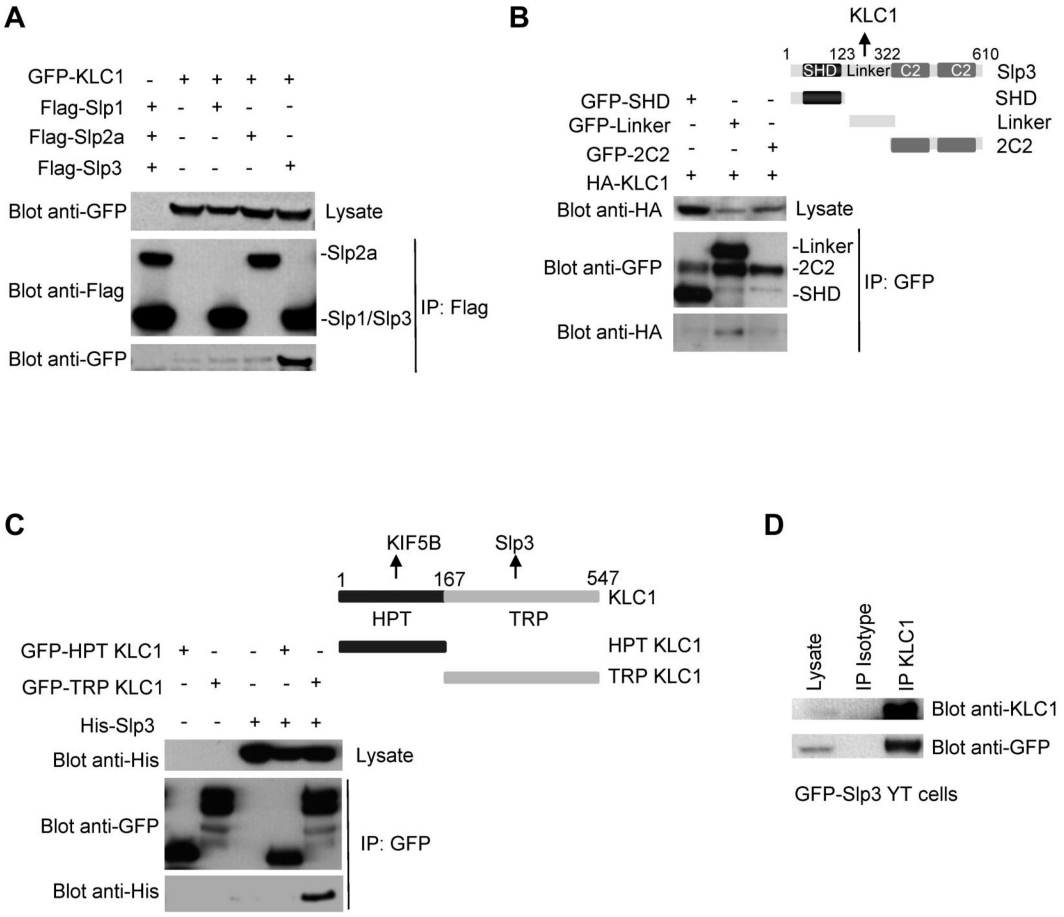

Figure 2. Mapping of the regions involved in the kinesin-1–Slp3 interaction

(A) Flag-Slp1, -Slp2, or -Slp3 and GFP-KLC1 were coexpressed into 293T cells. Cell lysates were immunoprecipitated with anti-Flag antibody and then separated by SDS-PAGE. Coprecipitated Slp proteins and KLC1 were immunoblotted with anti-Flag and anti-GFP antibodies. (B) For each Slp3 domain, a GFP fusion protein was cotransfected with HA-KLC1 into 293T cells. Cell lysates were immunoprecipitated with anti-GFP antibody and then separated by SDS-PAGE. Coprecipitated Slp3 domains and KLC1 were immunoblotted with anti-HA and anti-GFP antibodies. (C) GFP constructs of the N-terminal HPT or the C-terminal TRP were cotransfected with His-Slp3 in 293T cells. Cell lysates were immunoprecipitated with anti-GFP antibody. Coprecipitated Slp3 and KLC1 mutants were immunoblotted with anti-His and anti-GFP antibodies. (D) Cell lysates of a stable YT cell line expressing GFP-Slp3 construct were immunoprecipitated with an isotype control or with an anti-KLC1 antibody and immunoblotted with anti-KLC1 and anti-GFP antibodies. Blot results represent at least 3 independent experiments.

Europe PMC Funders Author Manuscripts

Europe PMC Funders Author Manuscripts

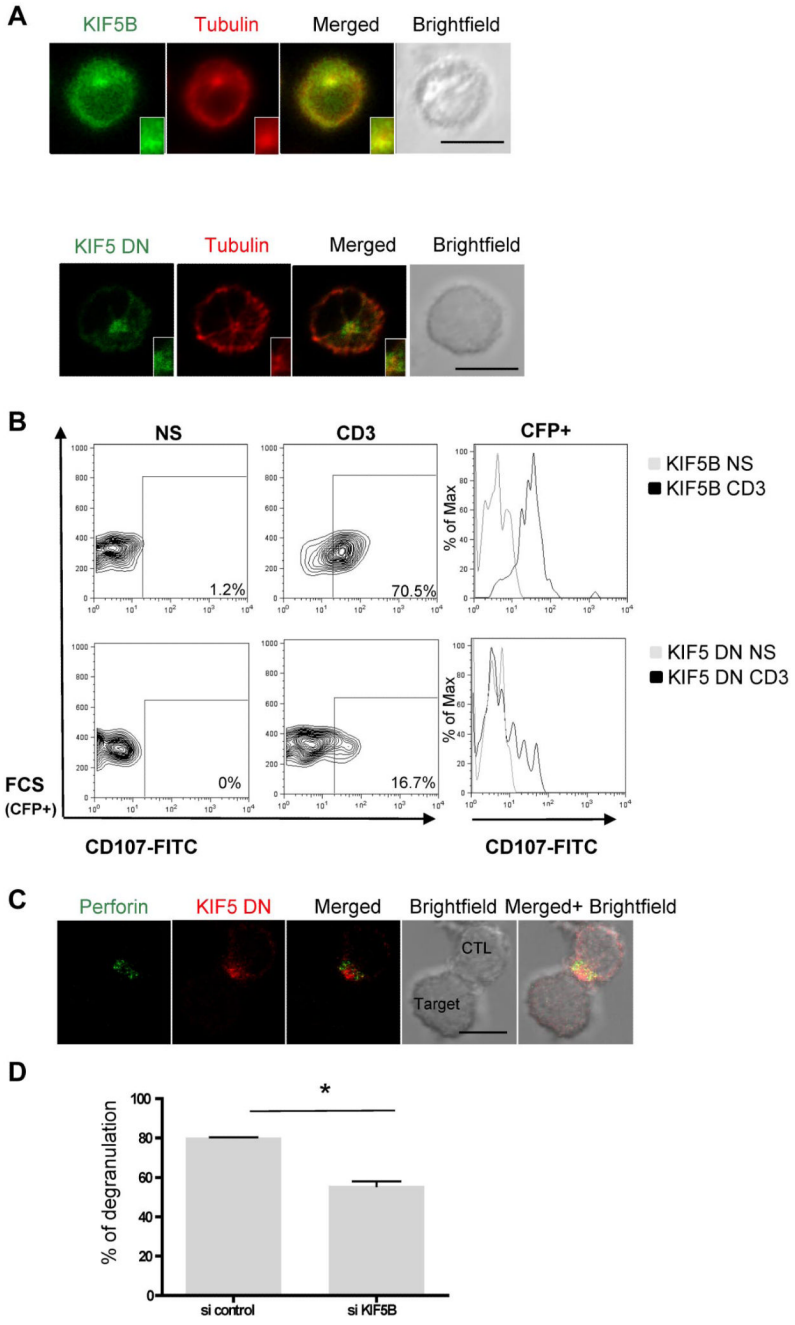

Figure 3. Kinesin-1 controls the terminal transport of lytic granules after granule polarization

(A) Top panel: confocal microscopy of CTLs transfected with GFPKIF5B. Cells were fixed, permeabilized, and stained with anti-tubulin (red). Bottom panel: confocal microscopy of CTLs transfected with GFP-KIF5 DN and stained with anti-tubulin (red). The insets represent an enlarged image. Scale bars represent 5 μm. All images of single cell were representative of > 60 cells observed over at least 4 independent experiments performed in duplicate. (B) Lak cells were transfected with CFP-KIF5B or CFPKIF5 DN. Transfected cells were incubated for 3 hours alone or with a coated anti-CD3 antibody in the presence of anti-CD107a–FITC and anti-CD107b–FITC antibodies. Thereafter, cells were stained with anti-CD3–PE and anti-CD8–APC antibodies. Lymphocytes were gated on $CD3^{+}CD8^{+}$ cells.

Profile shows CFP versus CD107-FITC gating on $CD3^+CD8^+$ CTLs. For each condition, a histogram overlay analysis of Lamp secretion by CFP^+ cells was performed. Each condition is representative of 3 independent experiments performed in duplicate. (C) Confocal microscopy of CTLs transfected with mCherry-KIF5 DN and conjugated with L1210 target cells. Cells were then fixed, permeabilized, and stained with anti-perforin antibody (green). Scale bars represent 5 μm. All images of conjugates were representative of > 90 cells observed over at least 3 independent experiments performed in triplicate. (D) CTLs cotransfected with CFP and siRNA control or siRNA targeting KIF5B were incubated for 3 hours alone or with a coated anti-CD3 antibody in the presence of CD107a and CD107b antibodies. CFP^+ cells were analyzed for Lamp secretion and shown in a representative histogram of 3 independent experiments. Statistical analysis was performed by Mann-Whitney test. $*P < .05$.

Europe PMC Funders Author Manuscripts

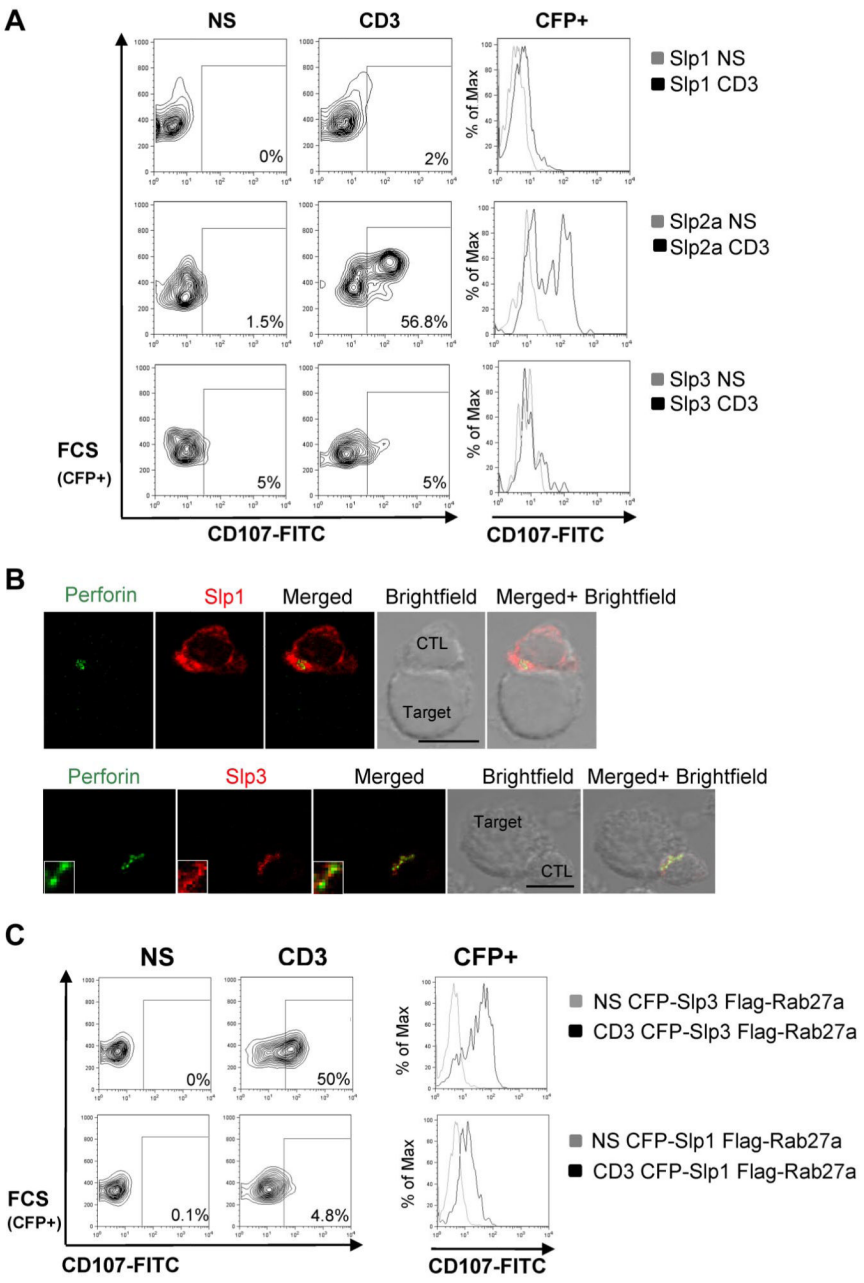

Figure 4. The Rab27a/Slp3 complex is involved in lytic granule secretion

(A) CTLs were transfected with CFP-Slp1, CFP-Slp2a, or CFP-Slp3 and then incubated for 3 hours alone or with a coated anti-CD3 antibody in the presence of CD107a and CD107b antibodies. Thereafter, cells were stained with anti-CD3–PE and anti-CD8–APC antibodies. Lymphocytes were gated on $CD3^+CD8^+$. The profile shows CFP versus CD107-FITC gating on $CD3^+CD8^+$ CTLs. For each condition, we perform a histogram overlay analysis of Lamp secretion by CFP^+ cells. Each condition is representative of 3 independent experiments performed in duplicate. (B) Confocal microscopy of CTLs transfected with DsRed-Slp1 or DsRed-Slp3 and conjugated with L1210 target cells. The cells were then fixed, permeabilized, and stained with anti-perforin antibody (green). The lower insets represent an

enlarged image. Scale bars represent 5 μm. All images of conjugates were representative of > 90 cells observed over at least 3 independent experiments performed in triplicate. (C) CTLs were transfected with CFP-Slp1 Flag-Rab27a or CFP-Slp3 Flag-Rab27a. Transfected cells were incubated for 3 hours alone or with a coated anti-CD3 antibody in the presence of CD107a and CD107b antibodies. Thereafter, cells were stained with anti-CD3–PE and anti-CD8p–APC antibodies. Lymphocytes were gated on $CD3^+CD8^+$. The profile shows CFP versus CD107-FITC gating on $CD3^+CD8^+$ CTLs. For each condition, we perform a histogram overlay analysis of Lamp secretion by CFP^+ cells. Each condition is representative of 3 independent experiments performed in duplicate.

Europe PMC Funders Author Manuscripts

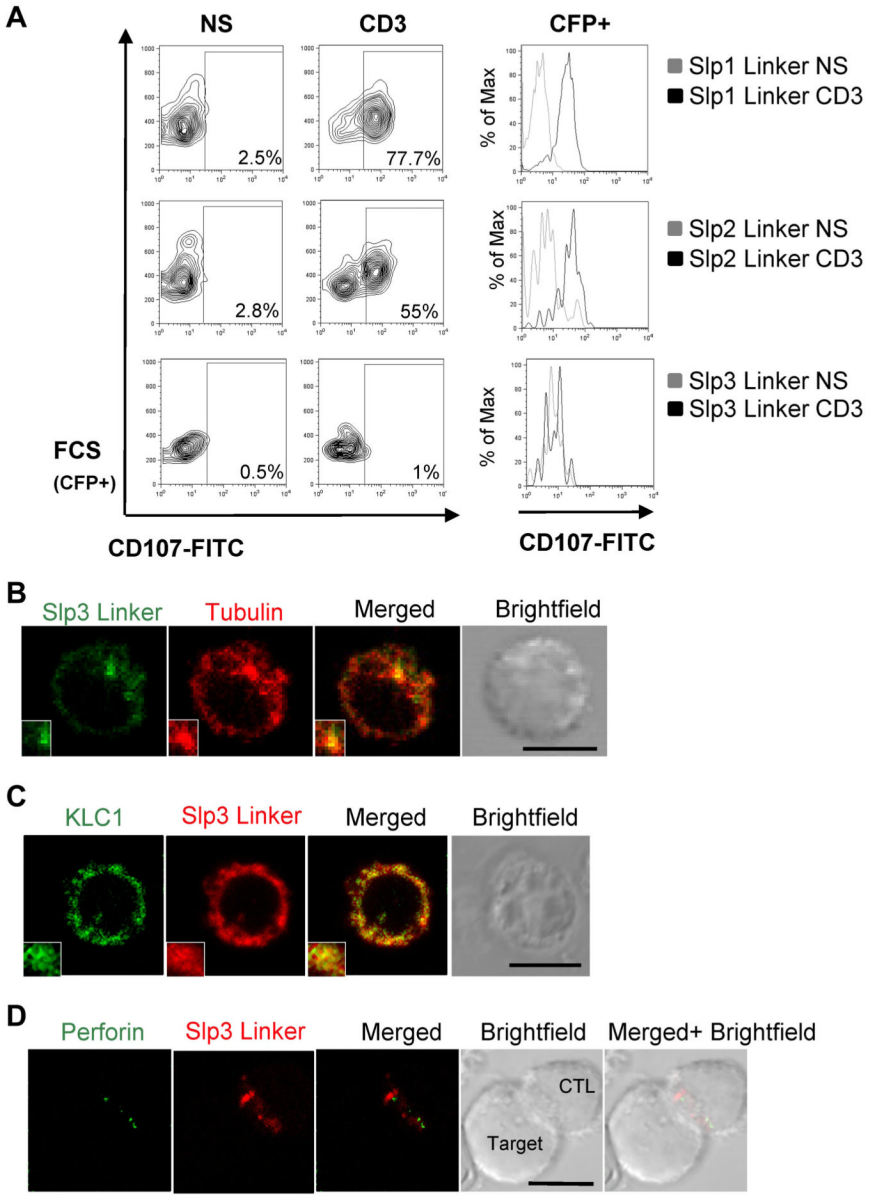

Figure 5. The Slp3-linker domain expression impairs Lamp release but has no effect on lytic granule polarization

(A) CTLs were transfected with CFP-Slp1 linker, CFP-Slp2 linker, or CFP-Slp3 linker. Transfected cells were incubated for 3 hours alone or with a coated anti-CD3 antibody in the presence of CD107a and CD107b antibodies. The cells were then stained with anti-CD3–PE and anti-CD8–APC. Lymphocytes were gated on $CD3^+CD8^+$. Profile shows CFP versus CD107-FITC gating on $CD3^+CD8^+$ CTLs. For each condition, we perform a histogram overlay analysis of Lamp secretion by CFP^+ cells. Each condition is representative of 3 independent experiments performed in duplicate. (B) Confocal microscopy of CTLs transfected with GFP-Slp3 linker and stained for α-tubulin (red). The insets represent an enlarged image. Scale bars represent 5 μm. All images of single cell were representative of > 60 cells observed over at least 4 independent experiments performed in duplicate. (C) Confocal microscopy of CTLs transfected with mCherry-Slp3 linker and GFP-KLC1. The

insets represent an enlarged image. Scale bars represent 5 μm. All images of single cell were representative of > 60 cells observed over at least 4 independent experiments performed in duplicate. (D) Confocal microscopy of CTLs transfected with mCherry-Slp3 linker and conjugated with L1210 target cells. Cells were then fixed, permeabilized, and stained with anti-perforin antibody (green). The insets represent an enlarged image. Scale bars represent 5 μm. All images of conjugates were representative of > 60 cells observed over at least 4 independent experiments performed in duplicate.

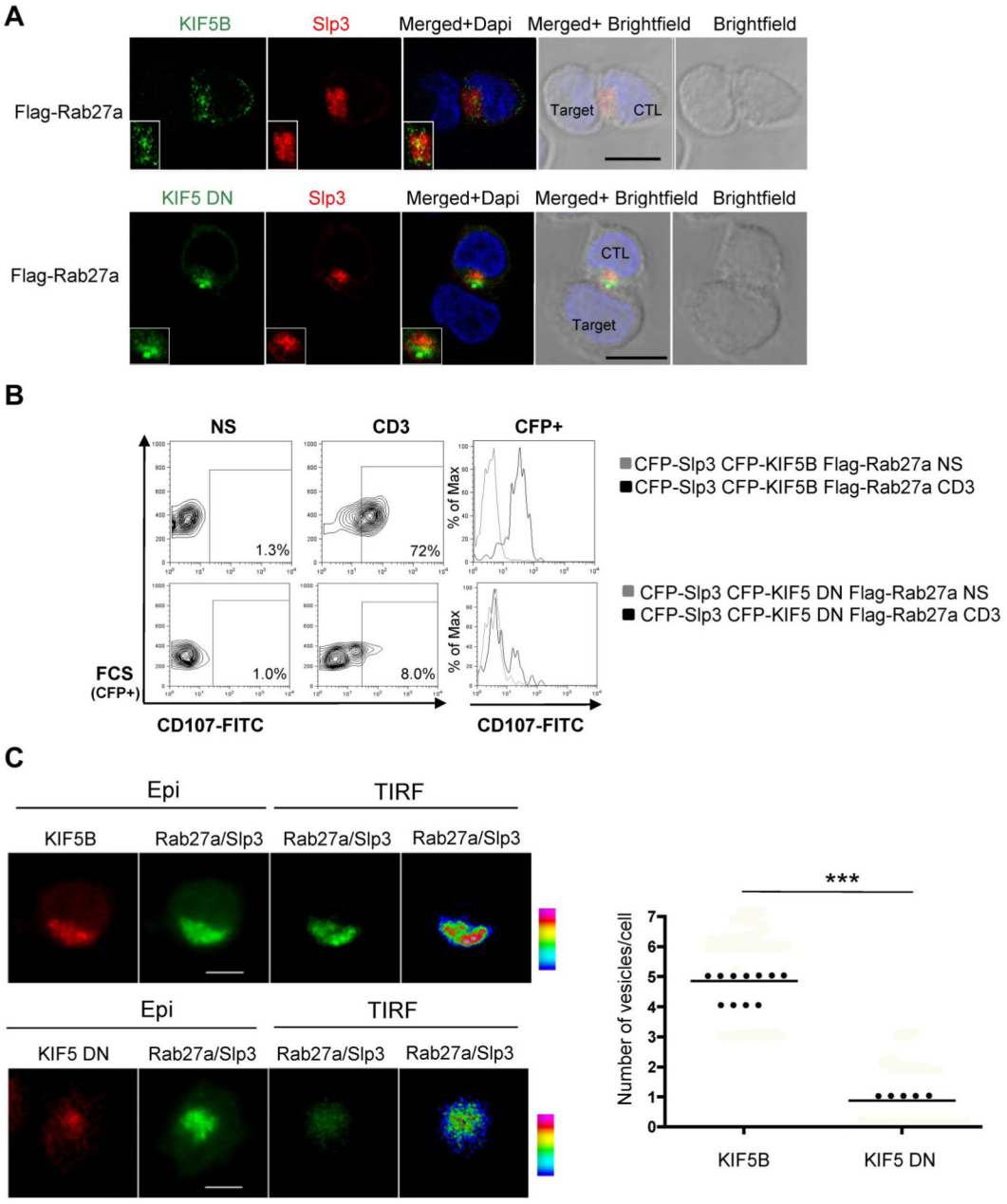

Figure 6. Kinesin-1 regulates the terminal transport of the Rab27a/Slp3 granules at the IS

(A) Confocal microscopy of CTLs transfected with GFP-KIF5B, DsRed-Slp3, and Flag Rab27a and conjugated with L1210 target cells (top panel, insets represent an enlarged image). Confocal microscopy of CTLs transfected with GFP-KIF5 DN, DsRed-Slp3, and Flag Rab27a and conjugated with L1210 target cells (bottom panel, insets represent an enlarged image). All images of conjugates were representative of > 90 cells observed over at least 3 independent experiments. (B) CTLs were transfected with CFP-Slp3, CFP-KIF5B, and Flag-Rab27a or CFP-Slp3, CFP-KIF5 DN, and Flag-Rab27a. Transfected cells were incubated for 3 hours alone or with a coated anti-CD3 antibody in the presence of CD107a and CD107b antibodies. The cells were then stained with anti-CD3–PE and anti-CD8–APC. Lymphocytes were gated on $CD3^{+}CD8^{+}$. Profile shows CFP versus CD107-FITC gating on

Europe PMC Funders Author Manuscripts

$CD3^+CD8^+$ CTLs. For each condition, we perform a histogram overlay analysis of Lamp secretion by CFP^+ cells. Each condition is representative of 2 independent experiments performed in duplicate. (C) Representative TIRF images of mCherry-KIF5B/GFP-Rab27a/GFP-Slp3 and mCherry-KIF5DN/GFP-Rab27a/GFP-Slp3 transfectant CTLs. The "pseudocolor" scales were used to indicate the intensity staining in TIRF. A vesicle was defined by a minimum of a square of 3 pixels per 3 pixels (1 pixel = 0.16 μm) of strong intensity signal (orange to purple). Scale bars represent 5 μm. The number of vesicles per cell acquired in TIRF mode is shown on the graph. Each dot represents an individual cell; and the line, the median value. For the mCherry-KIF5B/GFP-Rab27a/GFP-Slp3 condition, 20 cells have been analyzed from cumulating 3 independent experiments. For the mCherry-KIF5DN/GFP-Rab27a/GFP-Slp3 setting, 16 cells have been analyzed from cumulating 3 independent experiments. Statistical analysis was performed using a Mann-Whitney test. $^{***}P < .0001$.

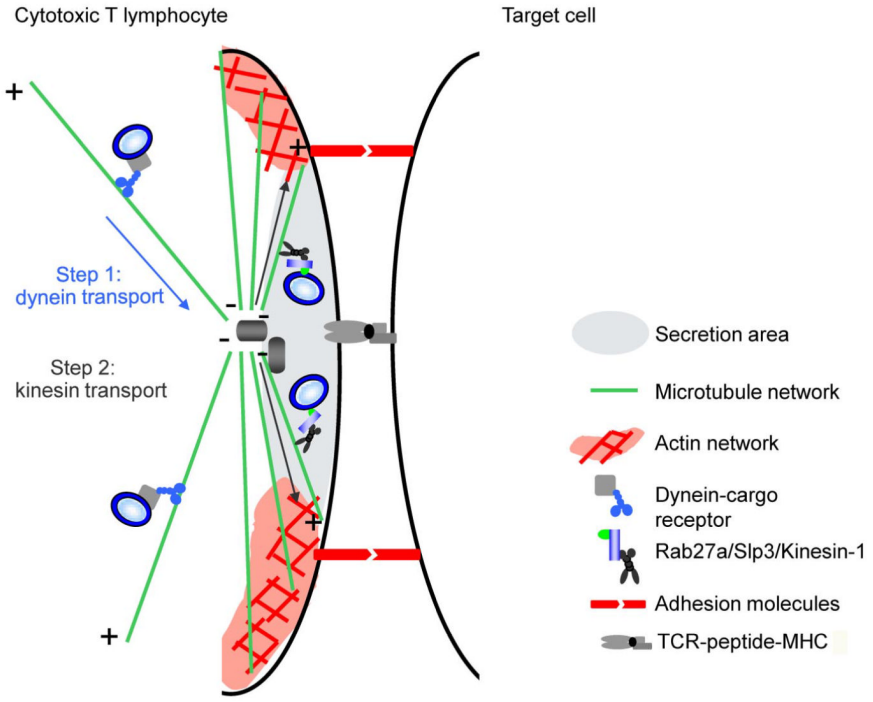

Figure 7. A model for lytic granule secretion at the IS

Secretion of cytotoxic granules at the IS involves 2 successive transport steps. First, a dynein-dependent transport step mediates the minus-end-mediated movement of cytotoxic granules to the MTOC.[8,9] Second, a plus-end kinesin-dependent transport step enables the polarized cytotoxic granules to reach the membrane and release their contents at the IS. In the latter step, granule-associated Rab27a recruits effector Slp3, which interacts with the kinesin-1 light chain (KLC1).

Europe PMC Funders Author Manuscripts